

Original

Sliding wear behavior of the WC/FeAl-B intermetallic matrix composites at high temperatures



Mohammad Mottaghi*, Mehdi Ahmadian

Department of Materials Engineering, Isfahan University of Technology, Isfahan 84156-83111, Iran

ARTICLE INFO

Article history:

Received 31 October 2019

Accepted 21 March 2020

Available online 25 April 2020

Keywords:

Wear-resistance

Intermetallic matrix composite

WC/FeAl-B composite

ABSTRACT

In this research, the sliding wear of sintered WC/40 vol% (FeAl-B) composites was studied at high temperatures. It is expected that the wear behavior of WC/FeAl can be improved in the presence of boron at high temperatures. The composites contained different amounts of boron and alumina was chosen as the counter body material in the wear tests. The tests were carried out at temperatures ranging from ambient to 600 °C so that the effect of boron and temperature on wear resistance could be specified. The results showed that while hardness slightly decreased with increasing the boron content to 500 ppm in the FeAl-B matrix, the fracture toughness increased significantly. The maximum wear resistance of the WC/FeAl-500 ppm B composite was recorded at all the temperatures examined. Investigations of the wear surfaces showed that while the wear mechanism of the WC/FeAl-B composites was an abrasive one at room temperature and 300 °C, a more adhesive wear mechanism was detected at 400 °C and a matrix oxidation mechanism was observed at 600 °C.

© 2020 SECV. Published by Elsevier España, S.L.U. This is an open access article under the CC BY-NC-ND license (<http://creativecommons.org/licenses/by-nc-nd/4.0/>).

Comportamiento de desgaste por deslizamiento de los compuestos de matriz intermetálica WC/FeAl-B a altas temperaturas

R E S U M E N

En esta investigación, se estudió el desgaste por deslizamiento de los compuestos sinterizados WC/40vol% (FeAl-B) a altas temperaturas. Se espera que el comportamiento de desgaste de WC/FeAl pueda mejorarse en presencia de boro a altas temperaturas. Los compuestos que contenían diferentes cantidades de boro y alúmina se eligieron como material del cuerpo del contador en las pruebas de desgaste. Las pruebas se llevaron a cabo a temperaturas que varían desde la temperatura ambiente hasta 600 °C, de modo que se pudiera especificar el efecto del boro y la temperatura sobre la resistencia al desgaste. Los resultados mostraron que si bien la dureza disminuyó ligeramente al aumentar el contenido de boro a 500 ppm en la matriz de FeAl-B, la tenacidad a la fractura aumentó significativamente. La resistencia al

Palabras clave:

Resistencia al desgaste

Compuesto de matriz intermetálica

WC/FeAl-B compuesto

* Corresponding author.

E-mail address: m.mottaghi@alumni.iut.ac.ir (M. Mottaghi).

<https://doi.org/10.1016/j.bsecv.2020.03.010>

0366-3175/© 2020 SECV. Published by Elsevier España, S.L.U. This is an open access article under the CC BY-NC-ND license (<http://creativecommons.org/licenses/by-nc-nd/4.0/>).

desgaste máxima del compuesto WC/FeAl-500 ppm B se registró a todas las temperaturas examinadas. Las investigaciones de las superficies de desgaste mostraron que, si bien el mecanismo de desgaste de los compuestos WC/FeAl-B era abrasivo a temperatura ambiente y 300 °C, se detectó un mecanismo de desgaste más adhesivo a 400 °C y se observó un mecanismo de oxidación de la

matriz a 600 °C.

© 2020 SECV. Publicado por Elsevier España, S.L.U. Este es un artículo Open Access bajo la licencia CC BY-NC-ND (<http://creativecommons.org/licenses/by-nc-nd/4.0/>).

Introduction

Cermets with a cobalt matrix have shown several restrictions like weak corrosion and oxidation resistance, high density and weak wear resistance. Besides, the mechanical properties of these hard metals decline significantly at high temperatures [1]. Metallic bearing materials such as cobalt, chromium, and molybdenum may lead to a series of complications [2].

Iron aluminides are strongly resistant to wear and erosion. Their wear resistance at high temperatures is higher in comparison with that of most binders like cobalt, nickel aluminides, and 304 stainless steel [3]. Furthermore, they offer good corrosion and oxidation resistance, high melting points and a rather low density while they can be manufactured at low costs. Due to these properties, iron aluminides have turned out to be suitable for structural applications under high temperature service conditions [4].

Recently, it has been proved that improvement in tribological traits of Fe₃Al compounds can be achieved by merging ceramic particles such as TiC, SiC, Al₂O₃, and TiB₂ [5–7]. Zhang et al. [8] showed the wear rate of the alloys is reduced by increasing the amount of TiC under similar empirical conditions, indicating that the addition of TiC hard particles enhances the wear resistance of the FeAl–Cr compound at high temperatures.

WC–FeAl and WC–Ni₃Al composites have been manufactured using the liquid phase sintering process under uniaxial pressure [9]. With the increase of the Ni₃Al content and also the sintering temperature, density and fracture toughness of cermets will increase and the porosity will decrease [10]. The sliding wear resistance of these cermets is especially influenced by their microstructural specifications such as form, structure, dimension and hard particle distribution in particular [11].

Mosbah and Wexler [12] investigated the wear behavior of the WC–FeAl composites at room temperature to find out that it was better compared to the WC–Co composites. They also considered that the fracture toughness of these hard metals was lower in comparison with that of WC–Co because of the low ductility of the FeAl matrix.

Generally speaking, the fracture toughness of aluminides can be increased through peripheral atmospheric control, microstructure control and heat treatment or by decreasing the particle size and adding alloying components [13]. In this relation, a method that has been newly employed to modify the composition of these materials involves the enhancement of the mechanical properties of the inter-metallics [14].

The reduction of tungsten carbide particle size enhances hardness. Newly, it has been proposed that by using extremely fine (smaller than 0.1 μm) particles of WC, dramatic improvements in wear behavior can be achieved [15–17]. Jianxin et al. [18] showed the wear rate of hard metals is enhanced with increasing the experiment temperature. They also showed that the cermet with the finest WC particles exhibited better wear behavior at temperatures up to 600 °C due to its greater hardness in comparison with the cermet with coarse WC particles.

Ahmadian et al. [19] presented the functional effects of boron in the sintered WC/FeAl-B composites and observed that increasing the boron quantities in such composites resulted in their greater toughness compared with the composites without boron due to the improved toughness of the FeAl binder. In another study of the abrasive wear of the WC/FeAl-B cermets at ambient temperature, the same authors discovered that the wear behavior of WC–FeAl would increase because of the addition of boron to the FeAl matrix [20].

During dry cutting or rapid machining with cermet devices, the temperature of the contact surface between the workpiece and the tool reaches to around 600 °C. The metal-ceramic composites start to oxidize at temperatures above 450 °C [21]. Hence, the friction and wear intensify and, consequently, the amount of wear will increase and the device durability will decrease [18].

Given the good strength of intermetallics at high temperatures, it has been proposed that they can enhance the wear behavior of the WC/FeAl-B composites when treated at high temperatures. The present study was designed and implemented to investigate the sliding wear of WC/FeAl-B cermets at high temperatures.

Experimental procedure

WC-40vol%FeAl cermets with various amounts of boron (from zero to 0.1 Wt.%) were prepared by uniaxial hot pressing of the particles under the liquid phase sintering condition at 1500 °C. Fe-40at%Al (FeAl) matrix alloys containing various amounts (0, 250, 500, 750 and 1000 ppm) of boron were produced by applying vacuum arc melting and chill casting under the argon atmosphere. Pure iron (Fe), aluminum (Al), boron (B) and WC (Sandvik Hard Materials, Sweden) were used. The elemental components with 99.9% or higher purity were utilized. Ingot melting, cutting, spinning, and blending were implemented several times to guarantee the homogeneity of boron.

The intermetallic ultrafine particles (<45 μm) were obtained by using a stainless steel ring grinding vessel under a specified helium inert atmosphere. The mixing of the FeAl-B with WC particles (0.69 μm) was done in a circular mill under a specified atmosphere. Induction heating was utilized under the controlled atmosphere and a loading of 20 MPa. All the cermets were sintered using a uniaxial hot press at 1500 °C for 4 min under a fractional argon atmosphere of approximately 10^{-2} Pa. Specimens of approximately complete density were fabricated for wear experiments using graphite dies with a 6.35 mm diameter [19].

Characterization of the composites

X-ray diffraction analysis (XRD, Philips X'Pert-MPD with $\text{Cu-K}\alpha$ radiation 1.54 Å, and a scan speed of 0.05°) was used for phase identification of these composites. Scanning electron microscopy (SEM, Philips, XL-Series) was applied for microstructural and morphological study of tungsten carbide particles in the specimens. Vickers hardness of the polished samples was specified via a macro-hardness tester (Otto Wolpert-Werke GMBH) under a load of 20 kg. The results of the hardness test were reported as the means of five test repetitions. The image analysis method was used to determine the indentation fracture toughness, K_{IC} , based on the measurements of the crack lengths resulted from the five test repetitions of Vickers hardness traces. Fracture toughness was calculated by applying the Anstis's formula [22]:

$$K_{\text{IC}} = 0.016(P)^{0.5} (1.5) \quad (1)$$

where E is the Young's modulus of the specimens, P is the indentation load, H is hardness and equals P/a^2 , a is the length of one side of the indentation and c is the length from one crack tip to the across from the crack tip divided by 2. Assuming a simple two phase composite, the Young's modulus was calculated from the following formula [1]:

$$E = \frac{[(C E_p E_m + E_m^2) (1+C)^2 - E_m^2 + E_p E_m]}{[(C E_p + E_m) (1+C)^2]} \quad (2)$$

where C is $(1/V_p)^{1/3} - 1$ with $V_p + V_m = 1$ (V_p and V_m are volume fractions of WC and FeAl, E_p is the Young's modulus of WC and equals 696 GPa [1]) and E_m is the Young's modulus of FeAl (261 GPa [23]).

Wear test

The composites were subjected to the sliding wear test by applying the pin-on-disk method at room conditions as per ASTM G 99-04 standard. The selected test method simulates the usage of these composites. The wear specimens comprised of cylindrical pins that were 6.35 mm in diameter. Al_2O_3 was chosen as the counter-face material because of its high mechanical and thermal stability at high temperatures up to 600 °C. The diameter of alumina disks (1700 HV) was 50 mm and their thickness was 5 mm and the average size of Al_2O_3 particles was measured to be about 200 μm . Using the control section of the software setup, the primary conditions for the tests were adjusted as reported in Table 1 (100 m sliding dis-

Table 1 – Conditions of the sliding wear tests at room and high temperatures.

Parameter	Regulated quantity
Vertical load	40 N
Sliding distance	100 m
Path radius	10 mm
Revolving velocity	60 rpm
Linear velocity	0.063 m s^{-1}
Roughness (pins)	$R_a = 0.183$, $R_q = 0.237$, $R_z = 1.075 \mu\text{m}$
Roughness (disk)	$R_a = 0.386$, $R_q = 0.464$, $R_z = 1.787 \mu\text{m}$
Relative humidity	Approximately 10%
Lubrication	Not used

tance belongs to the steady-state). The wear experiments were conducted under identical conditions to compare the samples results with each other. The wear experiments were accomplished at room temperature and also at 200, 300, 400, 500 and 600 °C. These conditions were selected according to the results of prior researches as they were practical with reference to the power of the apparatus and provided the demanded responsiveness in order to make distinctions among the mass losses of various samples.

The results of the wear tests were reported as the means of five test repetitions in the sense of the mass loss of each specimen. Before and after each experiment, the samples were soaked in acetone, cleaned ultrasonically, dried and weighted within ± 0.0001 g. Finally, the topography of the worn surfaces was observed by SEM.

Results and discussion

Characterization of the composites

The XRD patterns of WC-40 vol%(FeAl-B) composites are shown in Fig. 1. This figure demonstrates the main phases of WC, $\text{Fe}_{0.6}\text{Al}_{0.4}$, and FeAl_3 , and Fe_2Al_5 . Because of the low solubility of tungsten and carbon in FeAl without boron [24], no dissolved W or C was detected by X-ray diffraction. It can be seen that increasing the amount of boron up to 1000 ppm resulted in the broadening of the peaks of FeAl, which could be associated with the refining of the aluminide grains [25]. Also, there is a small shift in the lattice parameter of iron aluminide.

Fig. 2 shows the SEM back-scattered electron images of WC-40 vol%(FeAl-B) cermets. The bright areas are related to the WC powders and the black ones are attributed to the FeAl-B binder. In these images, the WC particles are seen to have a relatively uniform distribution in the matrix. It seems that tungsten carbide particles wet properly and that the intermetallic binders constitute a continual inter-granular phase. From a thermodynamic point of view, WC is congruous with Fe-40at%Al throughout the liquid phase sintering [26]. It can be seen that by adding some amounts of boron to the FeAl binder, the tungsten carbide particles in WC-FeAl-B became more flattened compared to the binder without boron. This improvement was attributed to the enhanced solubility of WC in the FeAl matrix in the presence of boron [25]. Moreover, boron is known to segregate at the grain boundaries of FeAl.

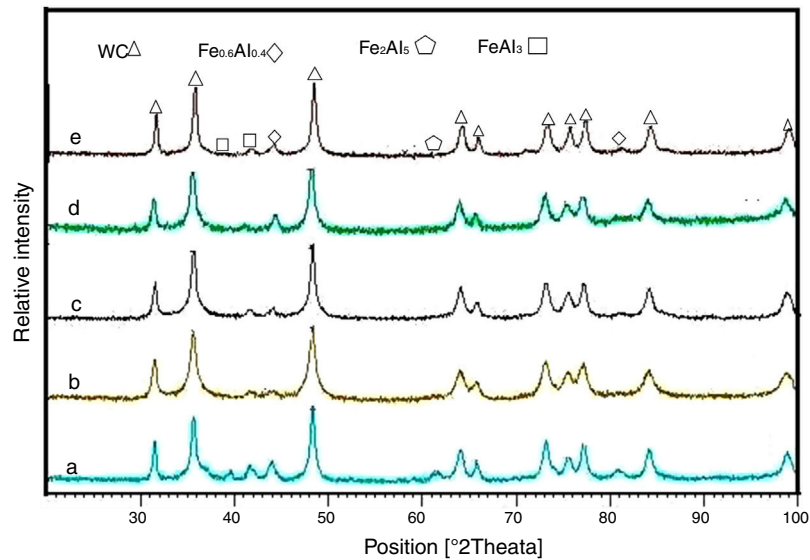


Fig. 1 – XRD patterns of WC/40 vol%(FeAl-B) with various contents of boron in the aluminide binder (a) 0, (b) 250, (c) 500, (d) 750 and (e) 1000 ppm B.

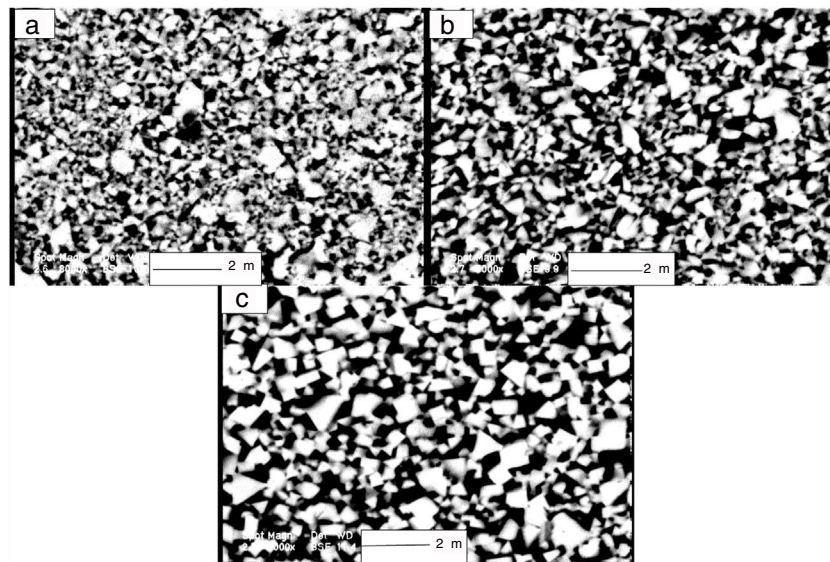


Fig. 2 – SEM backscattered electron micrographs of WC/40 vol%(FeAl-B) with various contents of boron in the aluminide binder (a) 0, (b) 500 and (c) 1000 ppm B.

This could affect the WC particle growth and prevent intergranular fracture of the intermetallic [27].

Fig. 3 illustrates the variations in the hardness and fracture toughness of the WC/ (FeAl-B) cermets by changing the boron content. (The error bars have been displayed for the chart with standard deviation). Clearly, the composites exhibited a slightly decreasing hardness with increasing the amounts of boron in the intermetallic binder. This could be attributed to the reducing hardness of iron aluminide with increasing the boron content [28].

Fracture toughness increased significantly with boron additions up to 500 ppm. Addition of more boron up to

1000 ppm, however, had no great impact on the fracture toughness.

It has been indicated that the toughness of the WC-FeAl cemented carbide can be raised by reforming the FeAl/WC interface in the presence of Cr, Zr, and B [1]. The enhanced fracture toughness of the WC-FeAl cemented carbide in the presence of boron maybe because of the effect of such factors as enhanced ductility, toughness and strength of iron aluminide, or maybe due to the enhanced tungsten carbide solubility in the iron aluminide matrix, decreasing of WC contiguity and aluminide grain size which leads to increased bond strength of the WC/FeAl interface [25]. This chain of causes

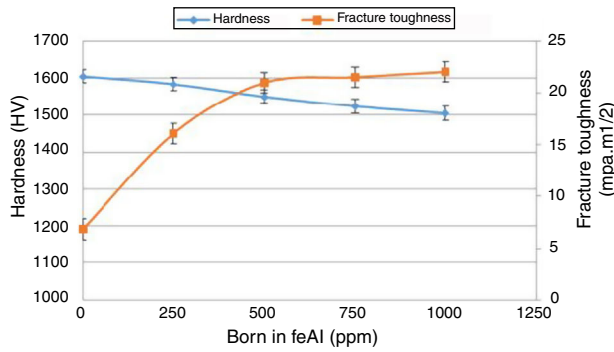


Fig. 3 – Effects of the amount of boron in the FeAl matrix on the hardness and toughness of WC/ (FeAl-B).

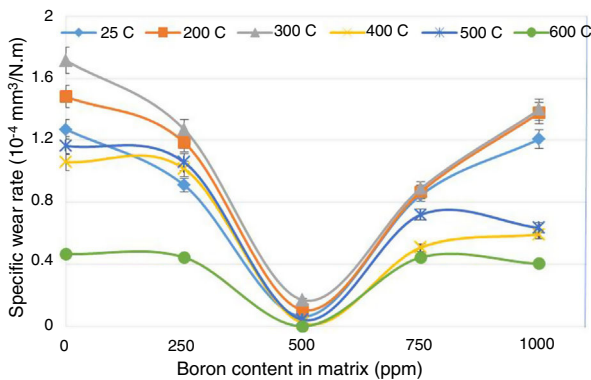


Fig. 4 – Effects of the amount of boron in the aluminide matrix on the specific wear rate of WC/ (FeAl-B) at different temperatures (°C).

results in an increased resistance against crack growth which, consequently, improves the fracture toughness of the carbide [27].

Wear resistance of the composites

Fig. 4 illustrates the variations in the specific wear rate of WC/ (FeAl-B) composites containing boron and treated at different temperatures. (The error bars have been displayed for the chart series with standard deviation). Firstly, it is obvious that the wear resistance of WC/ (FeAl-B) improved with increasing the boron content at all the specified temperatures. This is, of course, true for a boron content below 500 ppm beyond which it seems to have no significant, positive influence on the wear resistance of these composites. A slight enhancement in the boron content of FeAl leaves a great effect on the ductility of iron aluminide at low temperatures, apparently due to the strengthening influence of boron at the grain boundary [29,30]. It has been proved that boron segregates at grain boundaries in iron aluminide, which enhances the particle boundary cohesion and quickens sliding transmission across the grain boundaries [31]. An investigation has also shown that the presence of even trace amounts of boron increases the toughness of WC–FeAl composite, thus increasing the interface strength and wear resistance of the WC/aluminide cermets [25].

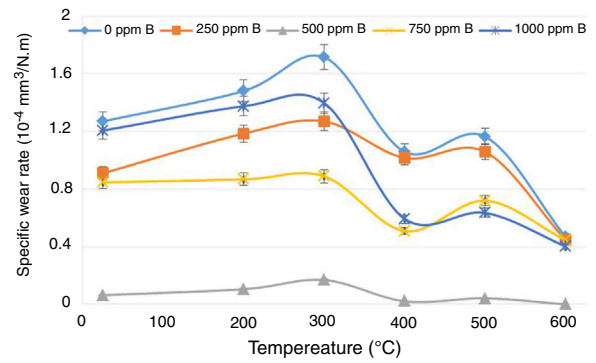


Fig. 5 – Effects of temperature on the specific wear rate in the WC/ (FeAl-B) cermets with various boron contents.

Secondly, the specific wear rate at high temperatures which get close to its value obtained at ambient temperature when the boron content is increased to 500 ppm. This represents the proper behavior of this composite at high temperatures. The third point that needs to be considered is the increasing specific wear rate by increasing the amount of boron from 500 to 1000 ppm. With the B increase up to 500 ppm, the fracture toughness significantly improves but after 500 ppm, it remains approximately stable while the hardness decreases. Therefore, it is expected that with the increase of B up to 1000 ppm, the wear resistance slightly decreases. Microstructure, carbide particle size and volume ratio of the matrix in the cemented carbides have an important effect on the wear resistance of cermets [32].

The specific wear rate of the WC/ (FeAl-B) cermets as a unit of temperature is observed in Fig. 5. (The error bars have been displayed for the chart series with standard deviation). The lowest and highest values of wear resistance at all temperatures were recorded for the specimens containing zero and 500 ppm of boron, respectively. The specific wear rate increased with increasing the temperature up to 300 °C because of the thermal collapse of the surface in all the specimens. At 400 °C, however, the specific wear rate declined probably due to the adhesion phenomenon (Figs. 8 and 12). Fractional oxidation of the surface at 500 °C leads to a slight adhesion (Figs. 9 and 12) so that the specific wear rate increases. Raising the temperature to 600 °C gives rise to the forming of an oxide layer on the surface of the specimens to decrease their specific wear rate again.

The friction coefficient of the WC/ (FeAl-B) composites as a unit of boron content and temperature are shown in Figs. 6 and 7 respectively. Increasing temperature up to 300 °C led to increase in the friction coefficients of the cermets because of the higher intensity of the wear surface contact. The friction coefficient decreased because of the reducing specific wear rate at 400 °C (Fig. 5). The friction coefficient illustrated an increasing trend when oxide particles formed and the cermets lost more of their masses at 500 °C. At 600 °C, an oxide layer formed on the surface of the cermets reducing the friction coefficient.

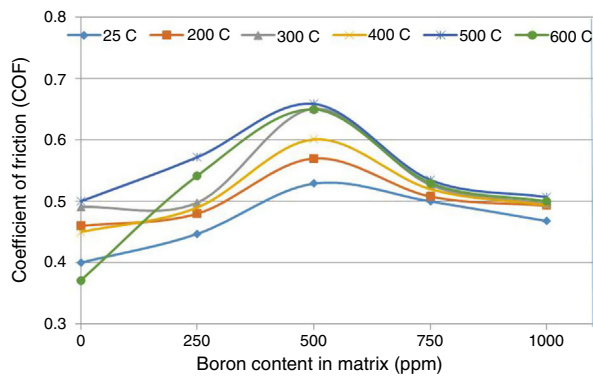


Fig. 6 – Effect of the amount of boron in the aluminide matrix on the friction coefficients of WC/ (FeAl-B) at different temperatures (°C).

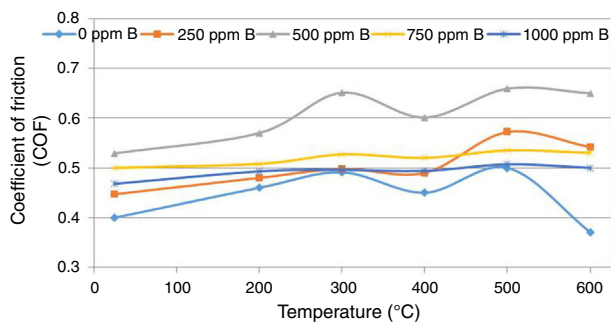


Fig. 7 – Effects of temperature on the friction coefficients in the WC/ (FeAl-B) cermets with various boron contents.

Wear surfaces

The SEM images of the worn surfaces of WC/FeAl-B cermets at room temperature are shown in Fig. 8. For the sample with no boron, wear occurred by forming craters at the junction

surfaces between the cermets and the disk. Concerning the higher hardness of the disk (1700 HV) compared with the WC/FeAl composite (1600 HV), the crater formation is probably caused by plowing. In this composite, micro-fractures were also detected on the worn surface. In the specimen with 500 ppm of boron, there was not any sign of the craters on the wear surface. The solution of boron in the FeAl binder resulted in a robust link at the binder and WC particles interface, thereby reducing the probability for the fragile fractures to form at the boundary of the binder and the reinforcement particles [28]. This changed the wear mechanism from a crater to an abrasive one. With increasing the boron content to 1000 ppm, the indentation fracture toughness remained constant but hardness decreased. The wear mechanism in this specimen was also identified as an abrasive one, but the depth of the wear abrasion was greater in comparison with the specimen containing 500 ppm of boron. In the absence of boron, the dominant mechanism was crater formation and removal of the brittle material. Finally, the WC-FeAl composite yielded a higher specific wear rate, which is in good agreement with the findings reported in Fig. 4. The same trend was observed at all the temperature range examined.

The SEM images of the worn surfaces of WC/FeAl-B cermets treated at 300°C are shown in Fig. 9. Several scratches, cracks, and particles can be seen pulling out on the worn surface (Fig. 9a). Particle de-bonding and pull out, binder extrusion, and band slipping are seen on the surface of the carbide particles (Fig. 9a). However, no trace of intense plastic deformation is observed in the wear surfaces (Fig. 9b and c). These two specimens have similar surface features (the rough wear track). These images are indicative of an abrasive wear mechanism. A comparison of these wear surfaces with those treated at ambient temperature reveals that they only differ in the enhanced abrasions and the area on which the abrasions have been developed. The wear mechanism of these composites at 300°C is the same as that at ambient temperature except for the higher specific wear rate of the former. This is verified by the specific wear rate results for all samples presented

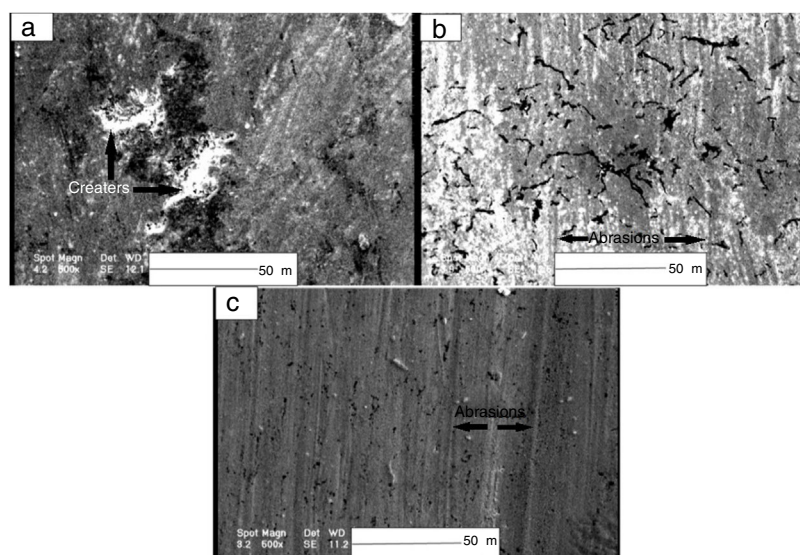


Fig. 8 – SEM secondary electron images of the worn surfaces for WC/FeAl-B at room temperature (a) 0, (b) 500 and (c) 1000 ppm B.

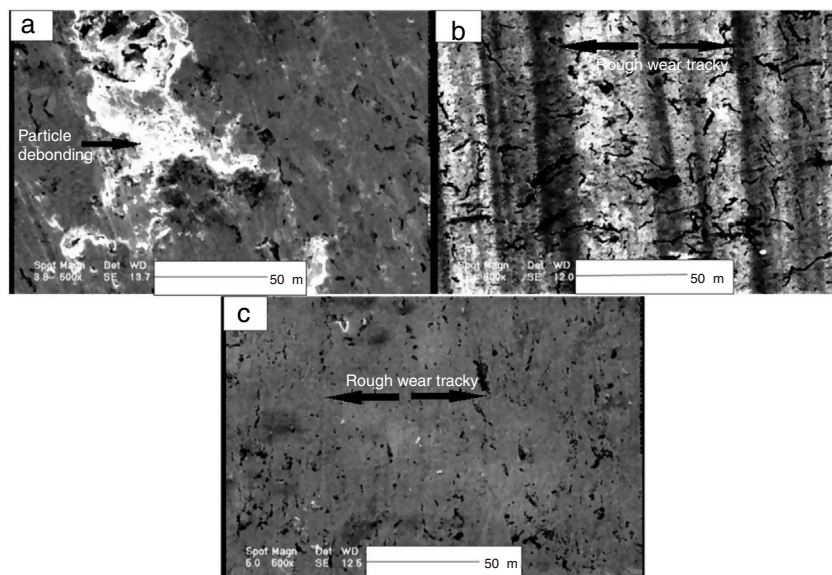


Fig. 9 – SEM secondary electron images of the worn surfaces for WC/FeAl-B at 300 °C (a) 0, (b) 500 and (c) 1000 ppm B.

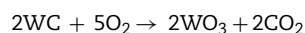
in Fig. 5. Finally, the specimen containing 500 ppm of boron exhibits the highest wear resistance because of its lower wear abrasion both in quantity and depth compared to the other cermets.

The SEM images of the worn surfaces of the WC/FeAl-B cermets at 400 °C are shown in Fig. 10. In the secondary electron images, an asperity is remarked on the specimens' wear surface which is the result of some debris from the disk adhering onto the pin. Thermal collapse takes place at this temperature on the surface of both the alumina disk and the composite pins. Consequently, throughout the sliding wear of the pin on the disk, some debris is separated from the surface of the disk and sticks onto the pin. Increasing of the temperature to 400 °C will lead to deeper and also a greater number of craters on the worn surface of the specimens. At this temperature, however, some debris from the disk seemingly filled in some parts of the craters, which decreased the specific wear rate in comparison to the conditions observed at 300 °C. Also, this is in good agreement with the specific wear rate results for all the samples presented in Fig. 5. Therefore, it seems that the dominant mechanism at this temperature is adhesion.

The SEM images of the worn surfaces of the WC/FeAl-B cermets at 600 °C are shown in Fig. 11. Increasing the temperature resulted in perfectly different wear surfaces. At this temperature, the worn surfaces morphology looks different from those at the lower temperatures. Here, the worn surfaces are relatively smooth and no craters are observed on the wear track. Furthermore, new oxide substances are observed in these images. Raising the temperature to 600 °C leads to the formation of an oxidative layer on the surface of the composites which naturally reduces the contact area between the pin and the disk throughout the sliding process. Therefore, the specific wear rate became smaller than that of the composite treated at 500 °C. This is approved by the specific wear rate results for all the samples presented in Fig. 5. The hill-like features observed in these images signify an oxidation mechanism.

Elemental analysis of the sample surfaces treated at various temperatures provides the information as to whether a physical or a chemical reaction has taken place. For this purpose, energy dispersive spectrometry (EDS) was used to analyze the elements of the adhered and non-adhered areas of the WC/(FeAl-B) composite surfaces treated at 400 °C. The results are shown in Figs. 12 and 13 for the specimens with 500 and 1000 ppm of boron, respectively. The percentage of Al is higher in the stuck areas than in the unstuck ones, showing the transmission of Al_2O_3 from the disk to the pin. Both morphologies are shown in Fig. 10 and the EDS results confirm an adhesive mechanism in operation at 400 °C. To investigate the oxide formation at 600 °C, the worn surfaces of the samples at room temperature and 600 °C were analyzed utilizing the EDS analysis [33]. The results of this analysis for the sample with 500 ppm of boron after treatment at ambient temperature have shown the wear grooves similar to those in Fig. 8b. A low and constant percentage of oxygen has been observed in all the areas of the specimen, indicating the formation of negligible oxide phases at ambient temperature. Abrasion can be observed in Fig. 8 and the analytical results are indicative of an abrasive mechanism for the WC/FeAl-B composites at ambient temperature [33].

The EDS results for the specimen without boron after treatment at 600 °C are presented in Fig. 14. The oxygen percentage in the oxide (darker) area is greater than that in the non-oxide areas, showing the existence of oxide substances in the darker area. The percentage of oxygen at ambient temperature is lower than that in the oxide area in the specimen treated at 600 °C. These observations indicate the possibility of the oxide phase formation at high temperatures. Another analysis shows that the wear surfaces include WO_3 after treatment at 600 °C [18]. WO_3 is considered to be a recently constituted phase due to the reaction of WC with O_2 . The reaction equation is expressed as follows [34]:



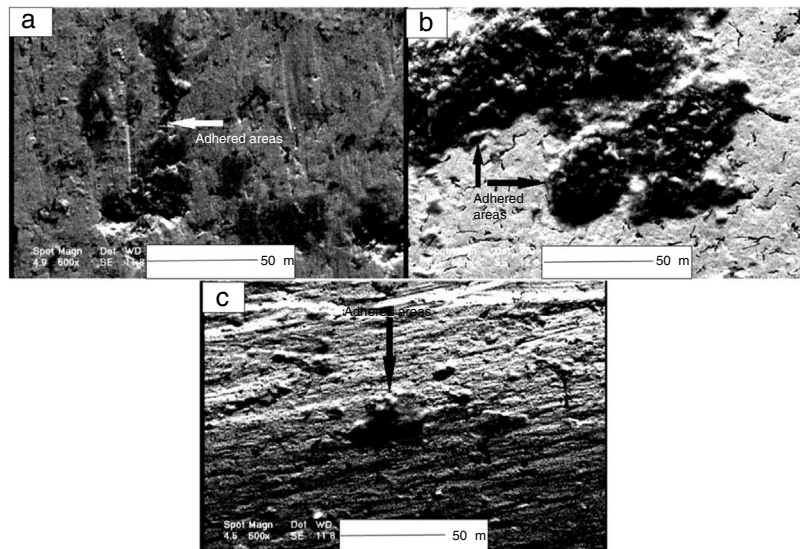


Fig. 10 – SEM secondary electron images of the worn surfaces for WC/FeAl-B at 400 °C (a) 0, (b) 500 and (c) 1000 ppm B.

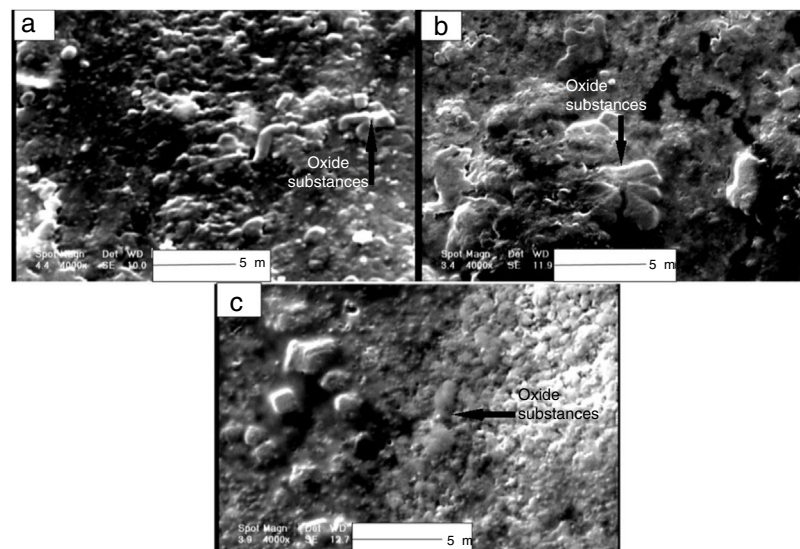


Fig. 11 – SEM secondary electron images of the worn surfaces for WC/FeAl-B at 600 °C (a) 0, (b) 500 and (c) 1000 ppm B.

The presence of oxides signifies an oxidation reaction taking place on the wear surfaces at high temperatures after treatment at 600 °C. The morphologies showed in Fig. 11 and the EDS results also indicate an oxidation mechanism at 600 °C [33]. The diversity in the characteristics of the WC-FeAl-B composite worn surfaces upon heat treatment at various temperatures is due to binder oxidation throughout wear experiments [18].

Different mechanisms seem to be involved in the removal of debris from the surface of the WC/FeAl-B cermets during the wear tests at ambient temperature [12,20]. In this study, the wear mechanisms including abrasion, particle ejection, matrix elimination, adhesion, and oxidation were remarked to be involved in debris removal from the WC/FeAl-B composites treated at different temperatures. Among these, matrix removal and particle pull out (for the WC-FeAl specimen) and abrasion (for the WC/FeAl-B specimen) were reckoned

to be the major ones involved at low temperatures (up to 300 °C) while the adhesive was the major wear mechanism at intermediate temperatures (400 °C). Finally, the oxidation wear mechanism was identified for the specimens treated at 600 °C. Generally speaking, some of the wear mechanisms work simultaneously and, therefore, have synergic effects on each other.

The significant wear resistance of these hard metals at high temperatures is required in many industrial applications like cutting tools, metal rollers, engine components, and mining tools.

Conclusions

In this study, the sliding wear behavior of tungsten carbide composites was investigated based on the intermetallic binder

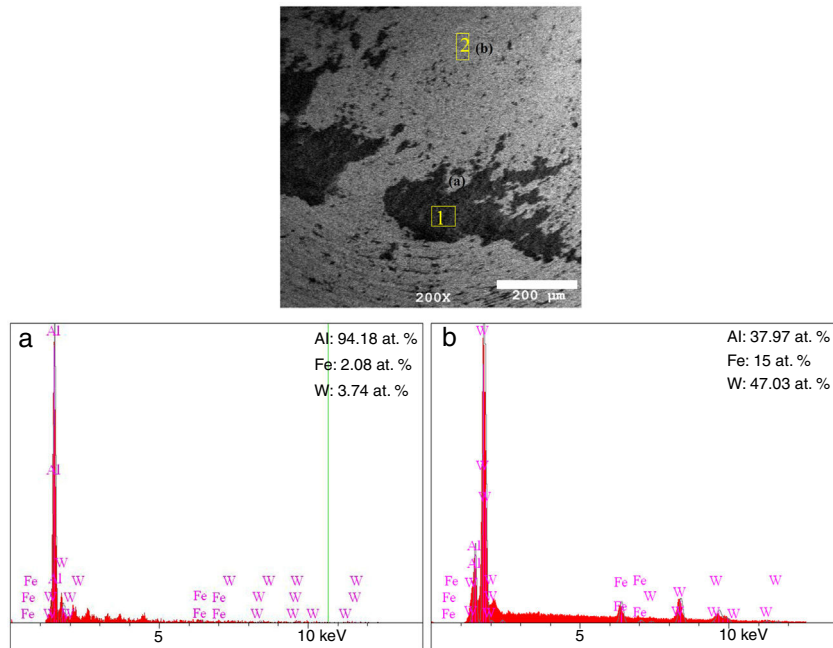


Fig. 12 – EDS analysis of the worn surfaces of the specimen with 500 ppm of B treated at 400 °C of the (a) stuck and (b) not stuck area.

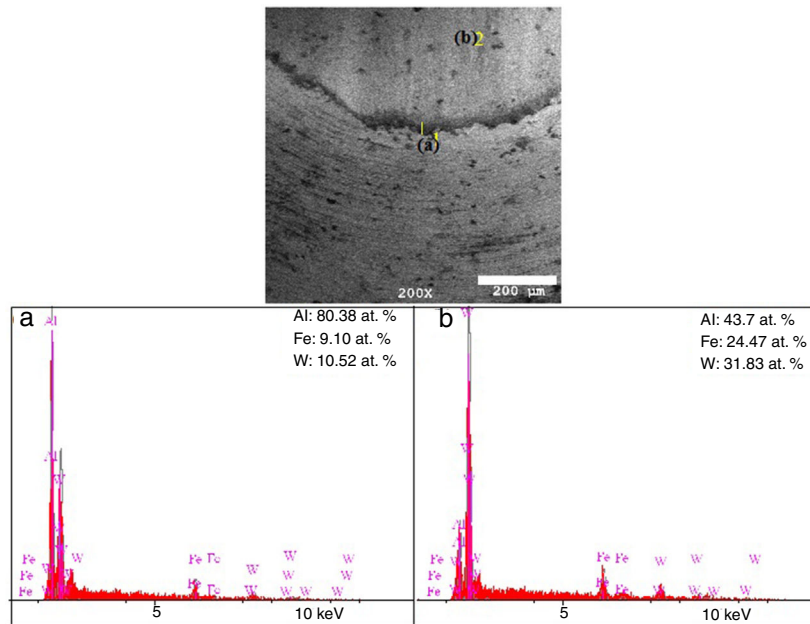


Fig. 13 – EDS analysis of the worn surfaces of the specimen with 1000 ppm of B treated at 400 °C of the (a) stuck and (b) not stuck area.

with and without boron at high temperatures ranging from 25 to 600 °C. The major findings of this research are as follows:

1. Boron addition up to 1000 ppm to the WC/FeAl-B composites leads to a slight decrease in hardness but a significant improvement in the fracture toughness.
2. The presence of boron up to 500 ppm in the WC/FeAl-B composites leads to significant improvements in the wear

behavior of the specimens at all the temperatures checked. This could be due to the optimum values of hardness and toughness and the different wear mechanisms that are simultaneously involved.

3. The wear mechanism of the WC/FeAl composite is accompanied by brittleness. In the presence of boron, on the other hand, the wear type is replaced by an abrasive one. This change could be related to the differences in the wear

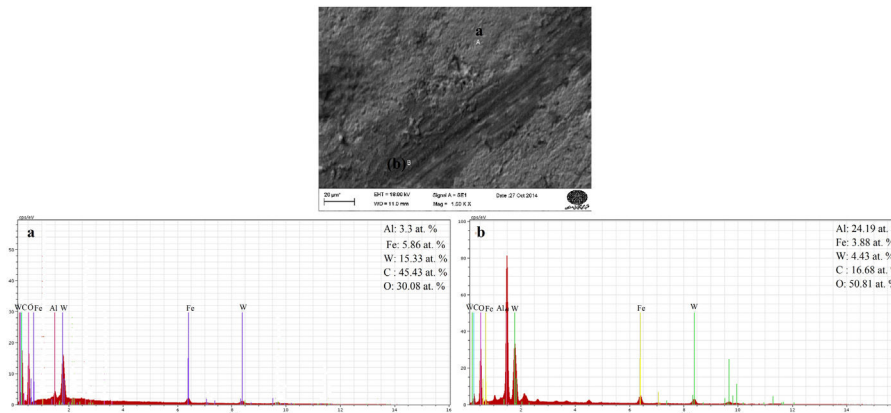


Fig. 14 – EDS analysis of the worn surface of the specimen without B of (a) non-oxide and (b) oxide area at 600 °C.

resistance of the composites. The wear mechanism of the WC/FeAl-B composites was found to be abrasive at room temperature and 300 °C. On the other hand, at 400 °C, the wear mechanism changes to adhesive whereas the oxidation mechanism was found to be dominant at 600 °C.

Funding

This research did not receive any specific grant from the funding agencies in the public, commercial, or not-for-profit sectors.

Conflict of interest

None.

REFERENCES

- [1] R. Subramanian, J.H. Schneibel, Intermetallic bonded WC-based cermets by pressureless melt infiltration, *Intermetallics* 5 (1997) 401–408.
- [2] W. Chen, H. Shi, H. Xin, N.R. He, W. Yang, H. Gao, Friction and wear properties of Si₃N₄-hBN ceramic composites using different synthetic lubricants, *Ceramics. Int.* 44 (2018) 16799–16808.
- [3] M. Johnson, D.E. Mikkola, P.A. March, R.N. Wright, The resistance of nickel and iron aluminides to cavitation erosion and abrasive wear, *Wear* 140 (1990) 279–289.
- [4] H.J. Grabke, Oxidation of NiAl and FeAl, *Intermetallics* 7 (1999) 1153–1158.
- [5] M. Inoue, H. Nagao, K. Suganuma, K. Niihara, Fracture properties of Fe-40at%Al matrix composites reinforced with ceramic particles and fibers, *Mater. Sci. Eng. A* 258 (1998) 298–305.
- [6] R. Subramanian, J.H. Schneibel, FeAl-TiC and FeAl-WC composites-melt infiltration processing, microstructure and mechanical properties, *Mater. Sci. Eng. A* 244 (1998) 103–112.
- [7] P. Malek, P. Kratochv, J. Pesicka, P. Hanus, I. Sediva, The nature of high-temperature deformation of the Fe₃₀Al₄Cr iron aluminide modified by TiB₂, *Intermetallics* 10 (2002) 985–992.
- [8] Z. Xinghua, M. Jiqiang, F. Licai, Z. Shengyu, L. Fei, Y. Jun, High temperature wear resistance of Fe-28Al-5Cr alloy and its composites reinforced by TiC, *Tribol. Int.* 61 (2013) 48–55.
- [9] A. Mosbah, D. Wexler, A. Calka, Tungsten carbide iron aluminide hardmetals: nanocrystalline vs microcrystalline, *Mater. Sci. Forum* 360–2 (2001) 649–654.
- [10] B. Huang, W. Xiong, Q. Yang, Z. Yao, G. Zhang, M. Zhang, Preparation, microstructure and mechanical properties of multicomponent Ni₃Al-bonded cermets, *Ceram. Int.* 40 (2014) 14073–14081.
- [11] J. Li, Y.C. Xia, The improvement of tribological behaviors of Cu-15%Al-4%Fe alloy by equal channel angular extrusion technique, *Mater. Des.* 30 (2009) 3076–3081.
- [12] A. Mosbah, D. Wexler, Abrasive wear of WC-FeAl composites, *Wear* 258 (2005) 1337–1341.
- [13] D.F. Johnson, E.A. Carter, First-principles assessment of hydrogen absorption into FeAl and Fe₃Si: towards prevention of steel embrittlement, *Acta Mater.* 58 (2010) 638–648.
- [14] N.V. Thuong, H. Zuhailawati, A.A. Seman, T.D. Huy, B.K. Dhindaw, Microstructural evolution and wear characteristics of equal channel angular pressing processed semi-solid-cast hypoeutectic aluminum alloys, *Mater. Des.* 67 (2015) 448–456.
- [15] S. Hiroyuki, I. Akira, S. Tomoharu, Effects of Co content and WC grain size on the wear of WC cemented carbide, *Wear* 261 (2006) 126–132.
- [16] K. Bonny, P.D. Baets, Y. Perez, J. Vleugels, B. Lauwers, Friction and wear characteristics of WC-Co cemented carbides in dry reciprocating sliding contact, *Wear* 268 (2010) 1504–1517.
- [17] J. Pirso, S. Letunovits, M. Viljus, Friction and wear behavior of cemented carbides, *Wear* 257 (2004) 257–265.
- [18] D. Jianxin, Z. Hui, W. Ze, L. Yansong, Z. Jun, Friction and wear behaviors of WC/Co cemented carbide tool materials with different WC grain sizes at temperatures up to 600 °C, *Int. J. Refract. Met. Hard Mater.* 31 (2012) 196–204.
- [19] M. Ahmadian, D. Wexler, A. Calka, T. Chandra, Liquid phase sintering of WC-FeAl and WC-Ni₃Al composites with and without boron, *Mater. Sci. Forum* 423 (2003) 1951–1956.
- [20] M. Ahmadian, D. Wexler, A. Calka, T. Chandra, Abrasive wear of WC-FeAl-B and WC-Ni₃Al-B composites, *Int. J. Refract. Met. Hard Mater.* 23 (2005) 155–159.
- [21] T. Zienert, M. Farhani, S. Dudczig, C.G. Aneziris, Coarse-grained refractory composites based on Nb-Al₂O₃ and Ta-Al₂O₃ castables, *Ceram. Int.* 44 (2018) 16809–16818.
- [22] G.R. Anstis, B.R. Lawn, D.B. Marshall, *J. Am. Ceram. Soc.* 64 (1981) 533.
- [23] J.H. Westbrook, R.L. Fleischer, *Basic Mechanical Properties and Lattice Defects of Intermetallic Compounds*, John Wiley, Chichester England, 2000.
- [24] S.L. Draper, D.J. Gaydos, M.V. Nathal, A.K. Misra, Compatibility of Fe-40Al with various fibers, *J. Mater. Res.* 5 (1990) 1976–1984.

- [25] M. Ahmadian, Sintering Microstructure and Properties of WC-FeAl-B and WC-Ni₃Al-B [Ph.D. Thesis], University of Wollongong, 2005.
- [26] A.V. Tumanov, Yu.V. Gostev, V.S. Panov, Yu.F. Kots, Wetting of TiC–WC system carbides with molten Ni₃Al, *Soviet Powder Met. Ceram.* 25 (1986) 428–430.
- [27] I. Baker, O. Klein, C. Nelson, E.P. George, Effects of boron and grain size on the strain-rate sensitivity of Fe-45A1, *Scr. Metall. Mater.* 30 (1994) 863–886.
- [28] M. Ahmadian, D. Wexler, A. Calka, T. Chandra, The effect of boron on the hardness and fracture toughness of WC-FeAl-B and WC-Ni₃Al-B composites, *Mater. Sci. Forum* 539 (2007) 962–967.
- [29] J.H. Schneibel, C.A. Carmichael, E.D. Specht, R. Subramanian, Liquid-phase sintered iron aluminide ceramic composites, *Intermetallics* 5 (1997) 61–67.
- [30] D.R. Joseph, J.L. John, Fracture toughness of monolithic nickel aluminide intermetallics, *Mater. Sci. Eng. A* 149 (1992) 143–151.
- [31] I. Baker, E.M. Sculson, J.R. Michael, R.A. Padgett, Grain boundary chemistry in Ni₃Al and Ni₃Si, *J. Phys. (Paris) Coll.* 1 (1990) 77–82.
- [32] T.E. Fischer, K. Jia, Abrasion resistance of nanostructured and conventional cemented carbides, *Wear* 200 (1996) 206–214.
- [33] M. Mottaghi, M. Ahmadian, Comparison of the wear behavior of WC/(FeAl-B) and WC-Co composites at high temperatures, *Int. J. Refract. Met. Hard Mater.* 67 (2017) 105–114.
- [34] S.N. Basu, V.K. Sarin, Oxidation behavior of WC-Co, *Mater. Sci. Eng. A* 209 (1996) 206–212.